

A Phase-Averaged Analysis of the Pedalling Cyclist Wake

T. N. Crouch¹, D. Burton¹, M. C. Thompson¹, D. T. Martin², N. A.T. Brown² and J. Sheridan¹

¹Fluids Laboratory for Industrial and Aerodynamic Research (FLAIR)
Department of Mechanical and Aerospace Engineering
Monash University, Clayton, Victoria 3800, Australia

²Australian Institute of Sport
Belconnen, Canberra 2616, Australia

Abstract

For a posture and pedalling frequency representative of an elite-level time-trialist, wind tunnel experiments show, perhaps for the first time, the changes to the wake flow topology over the course of a dynamic pedal stroke. Velocity field measurements are made in the wake of a full-size pedalling (100 RPM) mannequin in a time-trial position sitting on a bicycle. Using a phase-averaged approach, the wake structures passing through a downstream measurement plane are analysed as a function of crank cycle and are compared with similar wake measurements taken for static leg positions at fixed crank angles. It is found that the same fundamental fluid mechanisms that lead to the formation of the large-scale flow structure variants and wake asymmetries are consistent for both quasi-steady and dynamic pedalling conditions.

Introduction

In many cycling disciplines reducing aerodynamic drag is one of the most effective ways of improving athlete performance. In time-trial events, where high cycling speeds are achieved and sustained, the aerodynamic component of the resistive forces can account for up to 90% of the total resistance [5]. As a result, the power requirements of cyclists at racing speeds are essentially dictated by the magnitude of the aerodynamic resistance. Indeed, for races over relatively flat roads it has been shown that up to 96% of a cyclist's power is used to overcome aerodynamic drag [6]. Even small reductions in aerodynamic drag have been shown to have a significant impact on cycling performance [4]. Further improvements in aerodynamic performance are likely to arise from a better understanding of the three-dimensional flow around the complete rider bicycle system that incorporates the unsteady aerodynamics associated with the dynamic motion of the legs.

Recent experimental investigations into the aerodynamics of cyclists have provided insight into the flow structures around cyclist geometries [1, 2, 3]. Using a quasi-steady approach, Crouch *et al.* [1] mapped the time-averaged flow around the complete bicycle-rider system for various static leg positions. This was achieved through wind tunnel measurements with a full-scale cyclist mannequin in a representative time-trial position. (A similar mannequin geometry and position is used in this study.) It was revealed that the wake from the cyclist consists of multiple flow regimes and large streamwise trailing vortex systems, which are dependent on crank angle. For leg positions with aligned upper legs, corresponding to a horizontal crank, the wake showed reasonable symmetry relative to the mid-plane. As the legs were moved through the crank cycle, resulting in one leg being in an up and the other in a down position, large asymmetries in the trailing vortex wake developed. These asymmetries were associated with an increase in strengths of individual vortices in the large counter-rotating streamwise vortex pair and consequently in the aerodynamic drag. The degree of wake

asymmetry together with the strength of the primary vortices were found to account for much of the $\sim 20\%$ variation in the aerodynamic drag over the crank cycle. These findings on the effect of leg position were also predicted in a parallel computational study of Griffith *et al.* [7, 8].

Although the quasi-steady assumption does not seem unreasonable, given that the speed of the legs during pedalling is much slower than the forward motion of the cyclist, it is not clear that the effect of pedalling on the aerodynamics is negligible. One measure of the influence of the pedalling frequency f on the flow is through the reduced frequency. This is given in equation (1) as the ratio of the leg speed around the crank of length r , to the forward riding velocity U_∞ :

$$k = \frac{2\pi r f}{U_\infty}. \quad (1)$$

For elite-level cyclists riding over relatively flat terrain, typical values of the reduced frequency vary between 0.08 and 0.16. This study analyses the three-dimensional flow around a pedalling mannequin at a reduced frequency of $k = 0.11$ for a riding speed of 16 m/s at a cadence of 100 RPM. This investigation builds on the study of Crouch *et al.* [1] by quantifying the large-scale flow structures and asymmetries that develop in the wake, at the same Reynolds number, but under moving-leg conditions.

Method

Mannequin wake measurements were undertaken in the 2.0×2.0 m working section of the closed-circuit 450 kW wind tunnel at Monash University. The freestream test speed was 16 m/s, representative of a typical average cycling speed maintained in time-trial events at the elite level. The full-scale mannequin and cycling equipment, pictured in figure 1, is representative of the geometries and equipment used by elite-level male cyclists in a time-trial position. A more detailed description of the mannequin and cycling equipment is given in Crouch *et al.* [1]. The leg position during the crank cycle is described by the crank angle, with zero degree leg position corresponding to when the cranks are horizontally aligned and with the left leg in the downstream location. The 15° crank angle position is pictured in figure 1.

The mannequin/bicycle combination was rigidly fixed in the centre of the wind tunnel test section on top of a raised platform with struts attached to either side of the front and rear wheel axles. The raised platform was fitted with a cantilevered splitter plate that extended over the leading edge of the platform so as to limit the impact of the wind tunnel floor boundary layer on velocity field measurements. In this section of the tunnel the turbulence intensity is $< 1.4\%$ with a solid blockage ratio of 12%. Figure 2 shows the details of the setup of the mannequin in the wind tunnel.

The legs were driven through the fixed-gear bicycle drivetrain by rotating the rear wheel using a 200 watt DC electric motor. Both front and rear wheels were rotated via a friction drive mechanism housed underneath the wind tunnel floor. This consisted of the electric motor, which powered rollers positioned underneath each wheel, connected via a 1:1 belt-drive system. The legs were made to rotate at a representative elite-level cycling frequency of 1.67 Hz (100 RPM), with an accuracy of 0.02 Hz (± 1 RPM). At this cycling cadence and a bicycle gear ratio of 4.5 (54 tooth big chain ring and a 12 tooth rear sprocket), the wheel ground speed matched the wind-tunnel free-stream air velocity.

To investigate the validity of a quasi-steady assumption, detailed velocity fields were constructed for both static and pedalling conditions. Velocity field measurements captured the entire wake in a plane normal to the freestream flow one torso-length behind the mannequin (0.64 m). Time-averaged measurements of the three velocity components for static leg positions and phase-averaged for the dynamic leg conditions were obtained using a rake of four-hole dynamic pressure probes (Turbulent Flow Instrumentation Pty Ltd). The pressure probes have a frequency response of 2500 Hz, and are capable of measuring the three velocity component vectors to within 0.1 m/s and 0.1° for resultant velocities that lie within a $\pm 45^\circ$ forward-facing cone from the probe head. These measurements have been corrected for solid blockage effects using the correction methodology outline by Maskell [9].

The rake, consisting of four probes separated by 50 mm, was manoeuvred throughout the measurement plane using a motorised two-axis traverse. A total of 780 measurements were made across one half of the wake (shown in figure 2) with a minimum grid spacing of 25×25 mm in the core sections of the wake. Symmetry across the centre plane of the mannequin was assumed for leg positions 180° out-of-phase in order to reconstruct the entire left- and right-hand sides of the wake for both the static and pedalling conditions. This assumption was checked by comparing measurements made across the entire width of the wake at a number of heights for opposite leg positions. Time-averaged velocities from opposite sides of the symmetry plane for both static and pedalling cases were found to agree within 5% U_∞ .

Synchronised velocity and crank angle measurements allowed phase-averaged velocity fields within the measurement plane to be constructed and the structure of the pedalling cyclist wake to be analysed at various crank angles. The angle was determined



Figure 1. Mannequin position and cycling equipment.

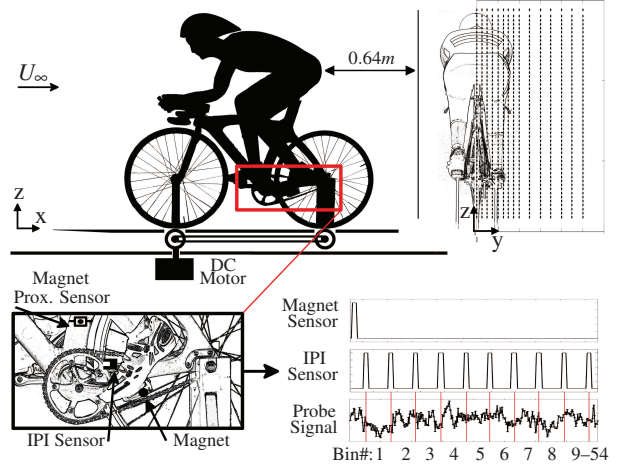


Figure 2. Side view of the setup of the pedalling mannequin. The rear view of the mannequin shows the velocity field measurement locations made in a plane a torso length (640 mm) behind the mannequin. The zoomed image of the crank shows the positioning of sensors used to determine the angle of the crank. This is shown along with an example of the phase-averaging process of probe data using signals output by these sensors. (Note: only the first 9 bins of a pedal stroke are shown for clarity).

in 54 intervals to within $\pm 0.25^\circ$ using an *inferred photo interrupter* (IPI) fixed to the bicycle frame that outputted a pulse signal as each tooth (1–54) of the large chain ring passed through the sensor. A magnet placed on the crank in combination with a magnetic proximity sensor fixed to the bicycle frame marked the beginning of each crank cycle. The magnet proximity sensor also served as a method of checking that all of the 54 pulses were received from the IPI sensor for each crank revolution. Phase-average measurements are a result of binning probe data in between the intervals at which the crank angle was determined, which corresponds to a bin size of 6.67° . An example showing the phase-averaging process is depicted along with the mannequin setup in figure 2.

For the pedalling experiments, the sample duration of velocity field measurements was 420 seconds (700 crank revolutions) in the most turbulent areas of the wake below the hips and 300 seconds (500 revolutions) for areas above the hips. The sampling frequency was 2500 Hz for these measurements. The sample time was selected so that the uncertainty ϵ associated with the variability of phase-averaged measurements in each bin was below 1.5% U_∞ at a 95% confidence level. The random variability associated with the phase-averaged data of each bin over the N crank revolutions is given by equation (2), where $z_c = 1.96$ for a 95% confidence level:

$$\epsilon = \frac{z_c \sigma_{bin\#}}{\sqrt{N}}. \quad (2)$$

Results

Due to the time taken for vortex structures to convect downstream from where they originate on the body of the mannequin to the measurement plane, the crank angle at which the phase-averaged results are depicted in this section have been offset to account for this lag. To compare static and dynamic leg results, an average convection velocity of $0.6U_\infty$ has been assumed, to calculate the phase-lag angle θ_{lag} using equation (3) below. In that case, l is the streamwise distance between the measurement plane and the point on the body where the vor-

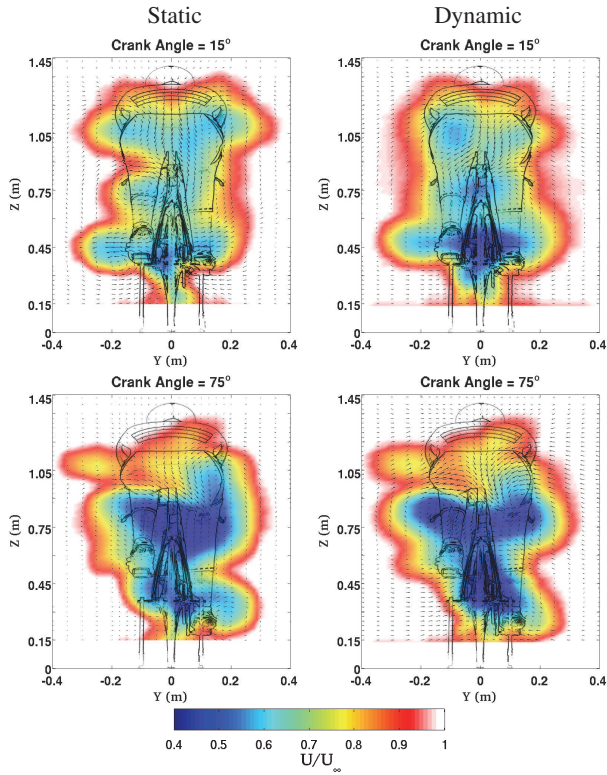


Figure 3. Contours of the time-averaged and phase-averaged streamwise velocity fields with in-plane velocity vectors overlaid for static and pedalling leg conditions respectively. The top row compares contours at the 15° symmetrical flow regime leg position and the bottom compares contours at the 75° asymmetrical flow regime leg position.

tices originate. This convection speed is in-line with other studies, which have found or have assumed similar estimates of the convection velocity in the wake of simple bluff body geometries such as circular cylinders [10]. Values typically range between 50–80% of the freestream velocity depending on whether the flow is investigated in the near or far wake regions. Although vortices present at various phases of the crank cycle will convect over a range of velocities, $0.6U_\infty$ is assumed to be a reasonable approximation, given that the core areas of the near wake, which are of most interest, are defined by regions where $0.4U_\infty < U < 0.7U_\infty$. Taking the streamwise distance between the measurement plane and the hip joint (0.7 m), where the dominant vortex structures originate, at a pedalling frequency of 100 RPM, the phase-lag is $\approx 45^\circ$. This has been assumed to be constant for the entire pedal cycle.

$$\theta_{lag} = \frac{2\pi l f}{0.6U_\infty}. \quad (3)$$

Both the time-averaged (static-legs) and phase-averaged (pedalling) velocity maps show the previously determined dominant features of the wake for the symmetrical and asymmetrical flow regimes as described by Crouch *et al.* [1]. Figure 3 shows contours of the streamwise velocity field for the symmetrical low-drag and asymmetrical high-drag leg positions. Good agreement is found in both the distribution and magnitude of the streamwise velocity field when comparing static and dynamic leg conditions. For the lower drag leg positions, corresponding to when the upper legs are approximately in alignment, represented here at the 15° crank angle, a near symmetrical wake profile is observed. As the legs proceed through the cycle, and

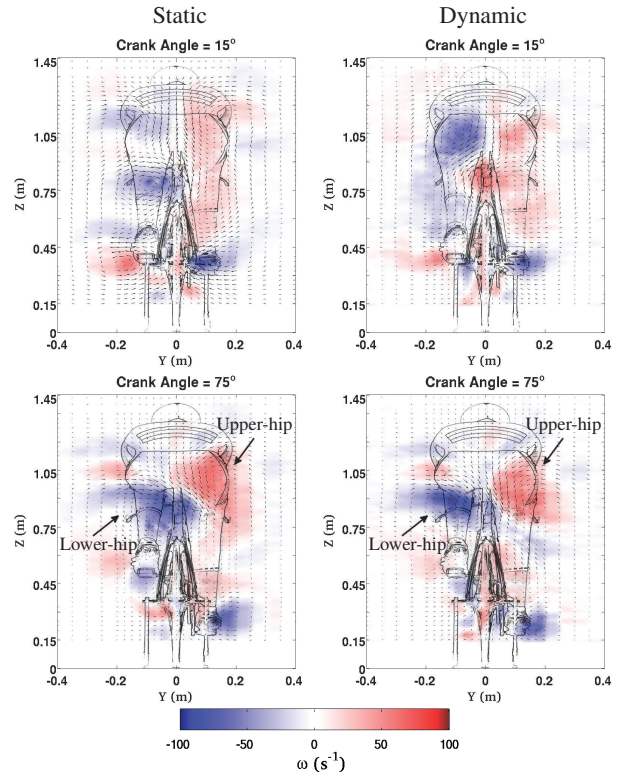


Figure 4. Contours of the time-averaged and phase-averaged streamwise vorticity fields with in-plane velocity vectors overlaid for static and pedalling leg conditions respectively. The top row compares contours at the 15° symmetrical flow regime leg position and the bottom compares contours at the 75° asymmetrical flow regime leg position.

the hip angle opens up, the wake undergoes transition to the higher drag asymmetrical flow regime. At these asymmetrical phases of the crank cycle, represented here at the 75° crank angle, both the static and dynamic leg results show the development of large deficits in streamwise velocity below the hips. These regions are where the largest changes in the wake velocity field occur throughout the crank cycle, and are associated with areas of the wake that contain the larger-scale and stronger vortex structures.

Figure 4 shows contours of the streamwise vorticity field for quasi-steady and phase-averaged conditions. Again, good agreement is found between static and pedalling leg results for both symmetrical and asymmetrical flow regimes. For leg positions of the symmetrical phases of the crank cycle, relatively weak streamwise vorticity magnitude is seen in the measurement plane. This is consistent with the findings of Crouch *et al.* [1], who showed for symmetrical leg positions there was a beneficial contraction in the size of the wake due to the mutual interaction of similar strength primary vortices of the same sign. For the asymmetrical leg positions as one leg is straightened and the other brought close to the chest, a slightly closer positional match in the streamwise vorticity and velocity fields is observed. For these more asymmetrical leg positions, which constitute the majority of the crank cycle, the time-averaged flow remains biased to one or other side of the wake.

For the asymmetrical 75° leg position, the formation of the large-scale wake vortices that persist downstream for the largest distance are clearly evident in both static and dynamic results. The contours of the streamwise vorticity field show the presence of a large counter-rotating vortex pair that is characteristic of the

high-drag asymmetrical flow regime. The upper hip vortex and the lower hip vortex, named after their point of origin and where they are positioned in the wake, are highlighted for both the static and moving-leg cases. The location, size and strength of these primary wake structures is consistent for both conditions. For this leg position it is seen the flow is directed across the body, due to the downwash generated between the vortex pair located towards the right-hand side of the wake. Vorticity shed downstream from other areas of the upper and lower body also compare well across the static and moving-leg vorticity fields. This was found not only for the 75° leg position depicted here, but for all leg positions characteristic of the asymmetrical flow regime of the crank cycle.

Velocity and vorticity fields also highlight lower areas of the cyclist wake that have previously not been analysed. Although the primary upper wake regions, as already discussed, are where the largest changes in the streamwise velocity and vorticity fields occur, there are still significant streamwise velocity defects in the lower wake. There is a widening of the wake in areas in-line with the rear wheel axle and the lower legs/feet for both the static and dynamic cases. The magnitude of the velocity deficit appears to be slightly more pronounced for the pedalling leg condition in this region. Smaller secondary wake structures are also observed in the lower wake for the 15° and 75° leg positions. In analysing the velocity field variation during the complete pedal stroke, these structures can be seen to follow the vertical displacement of the back of the ankle/calf as the leg moves through the crank cycle.

Conclusions

This experimental wind tunnel investigation has characterised the wake velocity deficit/streamwise vorticity distributions using phase-averaging. This has been done for realistic cycling cadences and racing speeds using a pedalling mannequin. It was shown that the primary features of the wake flow structures are consistent for both static and dynamic leg positions at the same crank angle. For pedalling phases corresponding to approximate alignment of the upper legs, a symmetrical flow regime was observed for both static and dynamic leg conditions. As the legs were moved through the crank cycle to the point that one of the legs straightened, the characteristic asymmetrical flow regime was observed. This was demonstrated for the high-drag 75° leg position, where the large-scale streamwise counter-rotating hip vortices were identified. The good agreement between the time-averaged static leg and the phase-averaged dynamic leg flow fields shows that the quasi-steady approximation, i.e., that the instantaneous near wake is the same independent of whether the legs are pedalling, is reasonable for a reduced frequency of up to 0.11 as investigated in this study. This covers a significant proportion of riding cadences and speeds typically achieved by elite cyclists in time-trial events. The upper limit of the reduced frequency at which the quasi-steady assumption starts to break down remains unknown.

Acknowledgements

The authors would like to thank Professor Simon Watkins for the loan of equipment used in this study. This research was partially funded by the Australian Research Council, through the Linkage Project scheme (project number: LP130100955).

References

[1] Crouch, T.N., Burton, D., Brown, N.A.T., and Thompson, M.C., and Sheridan, J., Flow topology in the wake of a cyclist and its effect on aerodynamic drag, *Journal of Fluid Mechanics*, **748**, 2014, 5–35.

- [2] Crouch, T.N., Burton, D., Brown, N.A.T., and Thompson, M.C., and Sheridan, J., Dominant flow structures in the wake of a cyclist, 30th AIAA Applied Aerodynamics Conference, New Orleans, USA, 2012.
- [3] Crouch, T.N., Burton, D., Brown, N.A.T., and Thompson, M.C., and Sheridan, J., A quasi-static investigation of the effect of leg position on cyclist aerodynamic drag, *Procedia Engineering*, **34**, 2012, 3–8.
- [4] Hosoi, A.E., Drag kings: characterizing large-scale flows in cycling aerodynamics, *Journal of Fluid Mechanics*, **748**, 2014, 1–4.
- [5] Kyle, C.R. and Burke, E.R., Improving the racing bicycle, *Mechanical Engineering*, **106(9)**, 1984, 34–45.
- [6] Martin, J.C., Milliken, D.L., Cobb, J.E., McFadden, K.L. and Coggan, A.R., Validation of a mathematical model for road cycling power, *Journal of Applied Biomechanics*, **14**, 1998, 276–291.
- [7] Griffith, M.D., Crouch, T.N., Thompson, M.C., Burton, D., Sheridan, J. and Brown, N.A.T., Computational Fluid Dynamics Study of the Effect of Leg Position on Cyclist Aerodynamic Drag, *Journal of Fluids Engineering*, **136(10)**, 2014, 101105.
- [8] Griffith, M.D., Crouch, T.N., Thompson, M.C., Burton, D., and Sheridan, J., Elite Cycling Aerodynamics: Wind Tunnel Experiments and CFD, Proceedings of the 18th Australasian Fluid Mechanics Conference, Tasmania, Australia, 2012.
- [9] Maskell, E.C., A theory of the blockage effects on bluff bodies and stalled wings in a closed wind tunnel, Tech. Rep. DTIC Document, 1963.
- [10] Wu, J., Sheridan, J., Welsh, M.C., and Hourigan, K., Three-dimensional vortex structures in a cylinder wake, *Journal of Fluid Mechanics*, **312**, 1996, 201–222.